VOLUME 68, NUMBER 22

JOC Articles

OCTOBER 31, 2003

Novel Crystal Structure, Cis−Trans Isomerization, and Host Property of Meta-Substituted Macrocyclic Azobenzenes with the Shortest Linkers

Yasuo Norikane, Kogorou Kitamoto, and Nobuyuki Tamaoki*

Institute for Materials and Chemical Process, National Institute of Advanced Industrial Science and Technology (AIST), 1-1-1, Higashi, Tsukuba, Ibaraki, 305-8565, Japan

n.tamaoki@aist.go.jp

Received January 28, 2003

Azobenzenophanes, in which two (**2**), three (**3**), and four (**4**) azobenzene units are connected cyclically by methylene linkers at the meta positions, were synthesized. The effect of ring strain on the structure and the photochemical and the thermal isomerization of azobenzene were investigated. Complex formation with guest species such as alkali metal cations and solvent molecules was observed. X-ray crystal analyses revealed the crystal structure of all three isomers of **2**. Compound **2**(t,c) was distorted due to the ring strain and **2**(c,c) was not deformed. Both **3** and **4** formed supramolecular channel structures in which an azobenzenophane molecule holds a solvent molecule in the molecular cavity. Upon exposure to light, **2**, **3**, and **4** exhibited stepwise trans−cis photoisomerization in solutions. The quantum yields for all isomerization steps of **2** were determined, and these values suggested that interactions between chromophores such as energy transfer and/or steric distortion affect the isomerization process. The lifetime of **2**(c,c) (19.7 days) was longer than that of **2**(t,c) (6.1 days) at room temperature. The relative stability of these isomers was explained by the isokinetic (or compensation) relationship between $\Delta H^{\ddagger}$ and $\Delta S^{\ddagger}$ values and by the effect of the ring strain. The relative energies of three isomers of **2** were estimated by HF/6-31G** calculations, and these values indicated that **2**(t,c) has the largest ring strain. Complexes (1:1 and 2:1) between macrocycles and alkali metal cations (Li^+, Na^+, K^+, Rb^+, Cs^+) were observed by ESIMS. The cation selectivity was shifted upon photoirradiation especially in **4**.

Introduction

Cis−trans photoisomerization of azobenzene is one of the typical photochromic reactions, and it has been of great interest in the development of light-driven functional molecules and materials such as photoresponsive host molecules,[1] polymers,[2] and liquid crystals.[3] In such systems, isomerization of azobenzene is often affected by steric distortion or the environment to which the azobenzene chromophore is exposed. In glassy polymer matrices, photo and thermal isomerizations of azobenzene do not follow the first-order kinetics due to the free volume in the matrices.[4] Bulky substituents[5] or cyclic structures[1,6] cause steric hindrance and alter the isomerization behavior. Azobenzenophanes, in which two azobenzene units are connected cyclically by two or three atomic chains, have been of interest in studying the effect of steric distortion on the photochemical cis−trans isomerization and the thermal stability of cis isomers.[6] Rau et al. synthesized an azobenzenophane (**1a**), in which two azobenzenes are connected by $-CH_2-S-CH_2-$ chains at

(1) (a) Shinkai, S.; Minami, T.; Kasano, Y.; Manabe, O. *J. Am. Chem. Soc.* **1983**, *105*, 1851−1856. (b) Vögtle, F. In *Supramolecular Chemistry: An Introduction*; John Wiley & Sons: Chichester, UK, 1989; Chapter 7.

(2) (a) Delaire, J. A.; Nakatani, K. *Chem. Rev.* **2000**, *100*, 1817−1845. (b) Hagen, R.; Bieringer, T. *Adv. Mater.* **2001**, *13*, 1805−1810. (c) Pieroni, O.; Fissi, A.; Angelini, N.; Lenci, F. *Acc. Chem. Res.* **2001**, *34*, 9−17.

(3) (a) Ichimura, K. *Chem. Rev.* **2000**, *100*, 1847−1873. (b) Tamaoki, N. *Adv. Mater.* **2001**, *13*, 1135−1147.

(4) (a) Yoshii, K.; Machida, S.; Horie, K. *J. Polym. Sci. Part B: Polym. Phys.* **2000**, *38*, 3098−3105. (b) Mita, I.; Horie, K.; Hirao, K. *Macromolecules* **1989**, *22*, 558−563. (c) Victor, J.; Torkelson, J. *Macromolecules* **1987**, *20*, 2241−2250.

(5) Rau, H. *J. Photochem. Photobiol. A: Chem.* **1988**, *42*, 321−327.

(6) (a) Rau, H.; Lüddecke, E. *J. Am. Chem. Soc.* **1982**, *104*, 1616−1620. (b) Tamaoki, N.; Koseki, K.; Yamaoka, T. *Angew. Chem., Int. Ed. Engl.* **1990**, *29*, 105−106. (c) Tamaoki, N.; Ogata, K.; Koseki, K.; Yamaoka, T. *Tetrahedron* **1990**, *46*, 5931−5942. (d) Tamaoki, N.; Yamaoka, T. *J. Chem. Soc., Perkin. Trans. 2* **1991**, 873−878. (e) Tamaoki, N.; Yoshimura, S.; Yamaoka, T. *Thin Solid Films* **1992**, *221*, 132−139. (f) Rau, H.; Röttger, D. *Mol. Cryst. Liq. Cryst.* **1994**, *246*, 143−146. (g) Röttger, D.; Rau, H. *J. Photochem. Photobiol. A: Chem.* **1996**, *101*, 205−214. (h) Tauer, E.; Machinek, R. *Liebigs Ann.* **1996**, 1213−1216. (i) Losensky, H.-W.; Spelthann, H.; Ehlen, A.; Vögtle, F.; Bargon, J. *Angew. Chem., Int. Ed. Engl.* **1988**, *27*, 1189−1191. (j) Funke, U.; Grützmacher, H.-F. *Tetrahedron* **1987**, *43*, 3787−3795. (k) Luboch, E.; Wagner-Wysiecka, E.; Kravtsov, V. C.; Kessler, V. *Pol. J. Chem.* **2003**, *77*, 189−196.

10.1021/jo0341160 CCC: $25.00
Published on Web 05/03/2003

the para positions to investigate the photoisomerization mechanism of azobenzene.[6a] Two different pathways have been proposed for the photoisomerization of azobenzene: the rotation mechanism and the inversion mechanism. They regarded that the rotation pathway was inhibited by the ring strain and demonstrated that the trans-to-cis photoisomerization from the $S_1(n,\pi^*)$ state of azobenzene occures along the inversion pathway instead of the rotation one, because the quantum yield of isomerization of **1a** from the trans,trans to trans,cis isomer (0.24) was similar to that of the trans-to-cis isomerization of azobenzene (0.23) on n,π^* excitation.[6a]

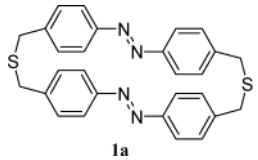

1a

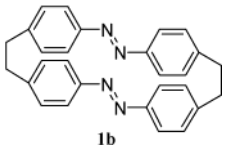

1b

The steric hindrance in azobenzenophanes also affects the rate of thermal cis-to-trans isomerization of azobenzene. Tamaoki et al. reported that an azobenzenophane, in which two azobenzenes are connected by $-CH_2-CH_2-$ chains at the para positions (**1b**), was unstable in the trans,cis isomer (τ = 22 s), although it was fairly stable in the trans,trans isomer (τ = 2.6 d).[6b,c] Thus, the photochemical formation of the cis,cis isomer was dependent on the light intensity, and Tamaoki et al. demonstrated that the compound could be used for photochromic memory with a nondestructive read-out property.[6d,e]

In the reported azobenzenophanes, which consist of two azobenzene units and two or three atomic chains between the azobenzene units, the rate of thermal cis-to-trans isomerization is affected by the position of the linkers and the chain length. When the azobenzene units are connected at the para positions (**1a**,**b**), the trans,cis isomer becomes very unstable, and the lifetime is up to seconds to minutes.[6a,b] On the other hand, the lifetime of the trans,cis isomer becomes longer than that of the cis,cis isomer when the azobenzene units are bridged at the ortho positions.[6h] As for the linkers at the meta positions, the syntheses of the compounds with two[6i] or three[6h] atomic chains have been reported; however, information on their physical properties, including thermal and photoisomerization, is lacking. No cyclic azobenzene dimer with linkers consisting of a single atom has been reported.

These investigations described above indicate that steric distortion affects the thermal isomerization as well as the photochemical isomerization properties of azobenzene. Thus, the knowledge of the correlation between the structure and the isomerization property of azobenzene may give information not only on the isomerization mechanism but also on a clue for controlling the photo and thermal cis−trans isomerization of azobenzene. However, the structure of the trans,cis or cis,cis isomers has not been revealed because of the thermal instability, although only the X-ray crystal structure of trans,trans isomers has been reported.[6c,7] As far as we know, there is only one recent report on the crystal structure of the cis isomer of macrocyclic azobenzenes.[6k] Host properties of azobenzenophanes have not been studied. Those compounds have a molecular cavity, and the size and shape of the cavity can be changed upon photoirradiation.

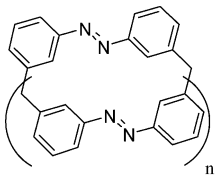

2; n = 2
3; n = 3
4; n = 4

In this study, we report the synthesis and properties of azobenzenophanes which contains two (**2**), three (**3**), and four (**4**) azobenzene units connected by linkers consisting of only one carbon atom at the meta positions. The purpose of this study is to investigate the correlation between the ring strain and the properties of azobenzene and to obtain preliminary data to evaluate the photoresponsive host properties of macrocyclic azobenzenes. As for **2**, the ring size is the smallest ever among the synthesized cyclic azobenzene dimers, and X-ray crystal analyses revealed the structure of **2**(t,t), **2**(t,c), and **2**(c,c), in some of which the *trans*- and *cis*-azobenzene units are sterically distorted. We have reported the preliminary results of the crystal structure of **2** as a communication.[8] The X-ray crystal structure analyses revealed the supramolecular channel structure of **3** and **4** where solvent molecules fit into the cavities of **3**(t,t,t) and **4**(t,t,t,t). The quantum yields for photochemical isomerization and the thermodynamic parameters for thermal isomerization among the three isomers of **2** were discussed from the viewpoint of the effect of the cyclic structure, such as steric distortion and/or interactions between the azobenzene chromophores, on the reactions. Electrospray ionization mass spectrometry (ESIMS) was applied to evaluate the host properties of **2**, **3**, and **4** versus alkali metal cations.

Results

Synthesis. Details of the synthesis of the macrocycles are described in the Experimental Section. A dilute solution of bis(3-nitrophenyl)methane[10] was added dropwise to a suspension of $LiAlH_4$ in dry 1,4-dioxane under a nitrogen atmosphere at 100 °C. The reaction mixture contained macrocycles with two (**2**(t,t)), three (**3**(t,t,t)), four (**4**(t,t,t,t)) azobenzene units, larger rings, and polymers. The "t" or "c" in the parentheses designate trans or cis configuration of the azobenzene moieties. These macrocycles were isolated by silica gel column chromatography, gel permeation chromatography (GPC), and recrystallization. Only the all-trans isomers were obtained by the reaction.

X-ray Crystal Structures. (a) Crystal Structure of 2(t,t). Recrystallization from dichloromethane/*n*-hexane mixture yielded red crystals suitable for the X-ray crystal structure analysis. The analysis revealed that there are two kinds of conformers (conformer A and B) in a unit

(7) Sawitzki, G.; Rau, H. *Liebigs Ann. Chem.* **1981**, 993−998.

(8) Norikane, Y.; Kitamoto, K.; Tamaoki, N. *Org. Lett.* **2002**, *4*, 3907−3910.

(9) (a) Lednev, I. K.; Ye, T.-Q.; Matousek, P.; Towrie, M.; Foggi, P.; Neuwahl, F. V. R.; Umapathy, S.; Hester, R. E.; Moore, J. N. *Chem. Phys. Lett.* **1998**, *290*, 68−74. (b) Nägele, T.; Hoche, R.; Zinth, W.; Wachtveitl, J. *Chem. Phys. Lett.* **1997**, *272*, 489−495. (c) Lednev, I. K.; Ye, T.-Q.; Hester, R. E.; Moore, J. N. *J. Phys. Chem.* **1996**, *100*, 13338−13341.

(10) Gattermann, L.; Rüdt, H. *Chem. Ber.* **1894**, *27*, 2293−2297.

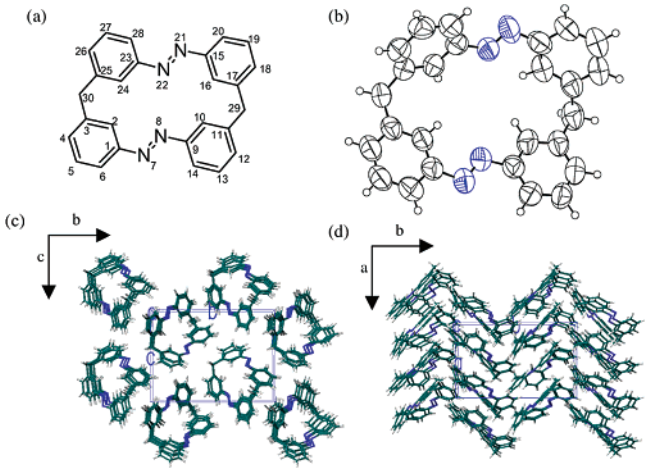

FIGURE 1. Chemical structure (a) and crystal structure of **2**(t,t). One of the two crystallographically independent molecules in **2**(t,t) (b) with displacement ellipsoids shown at the 50% probability level. The other molecule in **2**(t,t) was similar. Unit cell viewed along the *a*-axis (c) and along the *c*-axis (d).

TABLE 1. Torsion Angles and Bond Angle of Azobenzene Units of Macrocycles and Azobenzene

		CNNC	NNCC	NNC
trans				
trans-azobenzene[a]		180.0	17.4	114.1
2(t,t)	conformer A	−177.9	11, −10	108.6, 117.6
		168.3	9, −16	105.2, 114.0
	conformer B	174.1	−10, −5	108.2, 117.8
		170.6	−11, −19	109.0, 116.5
	calculated[c]	169.4	−29.8, 3.0	113.1, 117.7
2(t,c)	conformer C	−172	25, 1	109, 118
	conformer D	169	−27, 11	110, 117
	calculated[c]	−172.6	20.1, −9.6	111.3, 120.2
3(t,t,t)		−179	16, 13	106, 105
4(t,t,t,t)		176.8	−11.5, 5.8	113.7, 113.5
		−179.4	−3.8, 5.2	113.1, 114.9
cis				
cis-azobenzene[b]		8.0	53.3	121.9
2(t,c)	conformer C	−1	−51, −94	123, 125
	conformer D	6	54, 93	122, 123
	calculated[c]	−2.7	−58.8, 90.7	126.3, 125.7
2(c,c)		8.6	57.8	121.6
	calculated[c]	5.5	60.0	123.9

[a] Reference 11. [b] Reference 12. [c] Calculated by RHF/6-31G**

cell of **2**(t,t), while there are four molecules in a unit cell ($Z = 4$). One of the X-ray crystal structures (conformer A) of **2**(t,t) is shown in Figure 1b. The two conformers, A and B, are similar to each other, and both form a cone-like structure in which the benzene rings are tilted toward the inside of the cavity. The representative bond angles and torsion angles are compiled in Table 1. The torsion angles of N=N double bonds in conformer A are −177.9° and 168.3° for C1−N7−N8−C9 and C15−N21−N22−C23, respectively. The planes of the phenyl rings are twisted around the N=N−C planes. The torsion angles of the N=N−C=C bonds are 11°, −10°, 9°, and −16° for N8−N7−C1−C2, N7−N8−C9−C14, N22−N21−C15−C16, and N21−N22−C23−C28, respectively. These values indicate that not all the azobenzene units in **2**(t,t) are planar. The bond angles of N=N−C are bent toward the inside of the cavity; for example, N8−N7−C1 and N7−N8−C9 are 108.6° and 117.6°, respectively. The reported N=N−C angle in *trans*-azobenzene is 114.1°.[11] When a unit cell is viewed along the *a* axis, the molecules

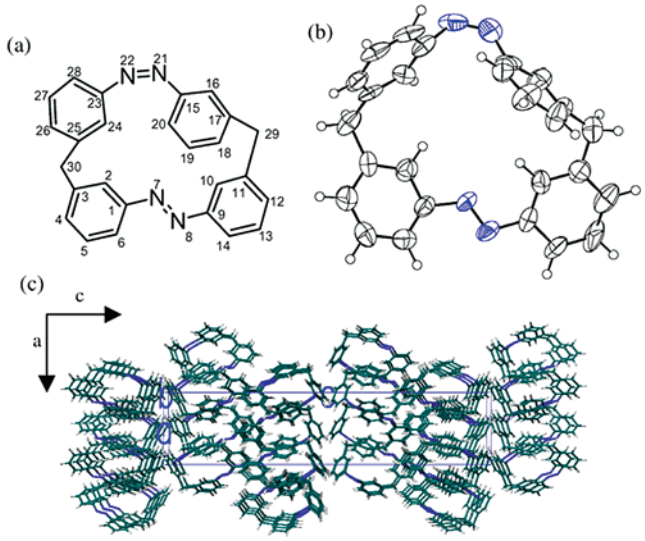

FIGURE 2. Chemical structure (a) and crystal structure of **2**(t,c). One of the two crystallographically independent molecules in **2**(t,c) (b) with displacement ellipsoids shown at the 50% probability level. The other molecule in **2**(t,c) was almost a mirror image of the molecule shown. Unit cell viewed along the *b*-axis (c).

form a channel structure. The unit cell is shown in Figure 1, parts c and d. In one column, two different conformers are aligned alternately. The molecular plane of **2**(t,t) is tilted about 30° versus the *a* axis.

(b) Crystal Structure of 2(t,c). The lifetime of **2**(t,c) was long enough for the isolation and recrystallization. As described in a later section, **2**(t,t) isomerized to give the trans,cis isomer (**2**(t,c)) followed by isomerization to the cis,cis isomer (**2**(c,c)) in acetonitrile, methanol, and benzene upon exposure to 313-, 366-, or 436-nm irradiation. **2**(t,c) was isolated on silica gel column chromatography from the solution at the 436-nm photostationary state. Recrystallization from methanol/dichloromethane mixed solvent gave orange crystals.

There are two different conformers (C and D) in a unit cell of **2**(t,c), while there are eight molecules in a unit cell ($Z = 8$). The molecular configurations of the two conformers, C and D, are almost mirror images of each other. One of the X-ray crystal structures (conformer C) of **2**(t,c) is shown in Figure 2b, and representative bond angles and dihedral angles are listed in Table 1. In the *trans*-azobenzene unit of conformer C, the dihedral angle of the C−N=N−C (C1−N7−N8−C9) bond is −172°, and the N=N−C=C bond angles are 1° and 25° for N8−N7−C1−C6 and N7−N8−C9−C10, respectively. The bond angles of N=N−C of the *trans*-azobenzene unit are bent toward the inside of the cavity; N8−N7−C1 and N7−N8−C9 are 118 and 109°, respectively. In the *cis*-azobenzene unit (conformer C), the dihedral angle of the C−N=N−C bond was −1° (C23−N22−N21−C15). The torsion angles of the N=N−C=C bonds are −51° and −94° for N22−N21−C15−C20 and N21−N22−C23−C24, respectively. It is notable that one benzene ring in the *cis*-azobenzene unit is perpendicular to the N=N−C plane. The N=N−C bond angles of the *cis*-

(11) Bouwstra, J. A.; Schouten, A.; Kroon, J. *Acta Crystallogr.* **1983**, *C39*, 1121−1123.

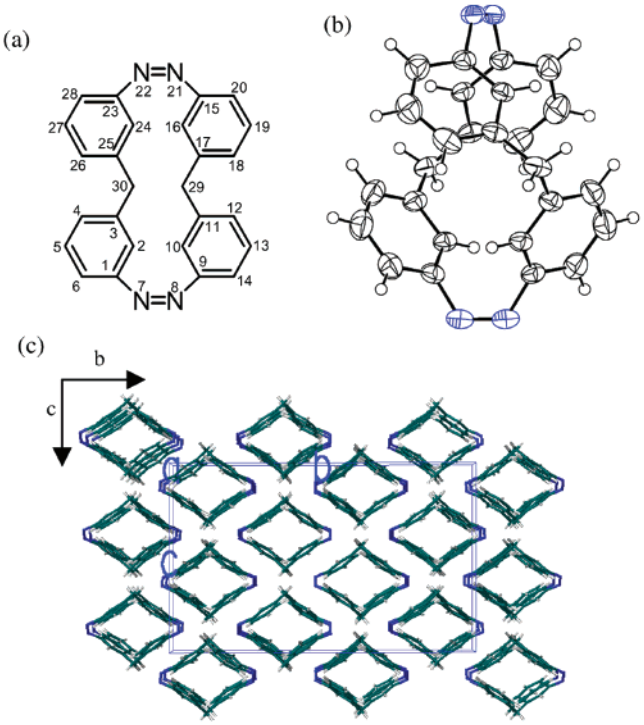

FIGURE 3. Chemical structure (a), crystal structure of **2**(c,c) with displacement ellipsoids shown at the 50% probability level (b), and unit cell viewed along the *a*-axis (c).

azobenzene unit are bent toward the outside of the cavity; N22−N21−C15 and N21−N22−C23 are 125 and 123°, respectively. The N=N−C bond angle in *cis*-azobenzene has been reported to be 121.9°.[12] As can be seen in Figure 2c, the channel structure was observed when the unit cell was viewed along the *b* axis. There are two kinds of columns in a crystal, and a single column consists of the same conformers.

(c) Crystal Structure of 2(c,c). **2**(c,c) was also stable enough for the isolation. Upon 366-nm irradiation of a highly concentrated methanol solution of **2**(t,t), crystals of **2**(c,c) were precipitated. Recrystallization from methanol/dichloromethane gave red crystals. The X-ray crystal structure of **2**(c,c) is shown in Figure 3b. There was only one conformer in the crystal. The molecule is highly symmetric and has D_2 symmetry with three 2-fold rotation axes. Thus, the shape of the two *cis*-azobenzene units is identical in a single molecule. The bond angle and dihedral angles are listed in Table 1. The torsion angle of the C−N=N−C bond is 8.6°. The planes of the phenyl groups are rotated around the N=N−C planes; the dihedral angle of N=N−C=C was 57.8°. The angle of the N=N−C bond was 121.6°. The crystal structure of the *cis*-azobenzene unit is close to that of *cis*-azobenzene in the literature; the torsion angles of C−N=N−C and N=N−C=C are 8.0° and 53.3°, respectively.[12] Thus, a *cis*-azobenzene unit in **2**(c,c) is not as distorted as that in **2**(t,c) in the crystal phase. The channel structure of **2**(c,c) is well aligned when the unit cell is viewed along the *a* axis as shown in Figure 3c.

(d) Crystal Structure of 3(t,t,t). Recrystallization of **3**(t,t,t) from chloroform yielded orange crystals, which

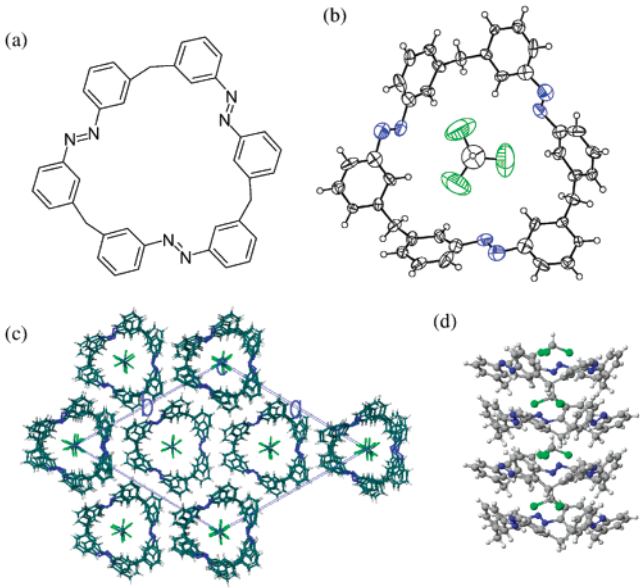

FIGURE 4. Chemical structure (a), crystal structure with displacement ellipsoids shown at the 50% probability level (b), unit cell viewed along the *c*-axis (c), and supramolecular channel structure (d) in **3**(t,t,t).

contained the solvent molecules in a 1:1 ratio as shown in Figure 4. The $CHCl_3$ molecule was located at the center of the molecular cavity of **3**(t,t,t). The complex has a 3-fold axis that was perpendicular to the molecular plane and passes the carbon atom of the chloroform molecule. Compound **3**(t,t,t) formed a bowl-like structure of which all the benzene rings of **3**(t,t,t) were tilted toward the inside of the molecular cavity and faced the $CHCl_3$ molecule. The chlorine atoms of chloroform pointed toward the benzene rings. The angle of the C−Cl bond of chloroform and the plane of the benzene ring was about 60°, and the distance between the chlorine atom and the benzene ring was 3.4 Å. The twist angle of the C−N=N−C bond of an azobenzene unit was −179°. The torsion angles of the N=N−C−C bond were 16° and 13°, respectively. The supramolecular channel structure was observed along the *c* axis. The molecular plane of **3**(t,t,t) was perpendicular to the *c* axis and parallel to the a−b plane. In one column, the carbon atoms of the chloroform molecules were located along a straight line. The distance between the chloroform molecules was 4.69 Å.

(e) Crystal Structure of 4(t,t,t,t). The crystal of **4**(t,t,t,t) was obtained by recrystallization from dichloromethane. The crystal was the 1:1 complex of **4**(t,t,t,t) with the solvent molecule, and it also formed a supramolecular channel structure as shown in Figure 5. The shape of the **4**(t,t,t,t) molecule looks like stitches on a tennis ball. The dichloromethane molecule was surrounded by four azobenzene units. The complex had a 2-fold axis that passes through the two chlorine atoms of the dichloromethane molecule. The position of the $-CH_2-$ moiety of the CH_2Cl_2 molecule has two possibilities with equal probabilities according to the symmetry of the complex. The twist angles of the C−N=N−C bond of an azobenzene unit were −179.4° and 176.8°. The torsion angles of the N=N−C−C bond are in the region of 3.8−11.5°. The benzene rings did not face the solvent

(12) Mostad, A.; Rømming, C. *Acta Chem. Scand.* **1971**, *25*, 3561−3568.

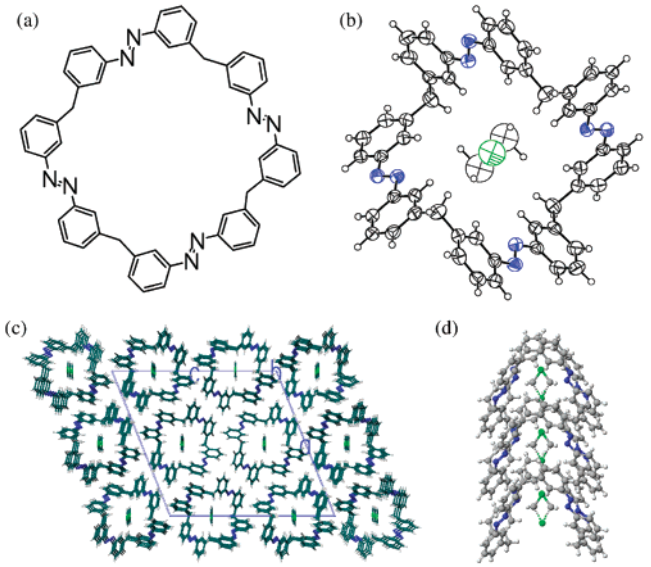

FIGURE 5. Chemical structure (a), crystal structure with displacement ellipsoids shown at the 50% probability level (b), unit cell viewed along the *b*-axis (c), and supramolecular channel structure (d) in **4**(t,t,t,t).

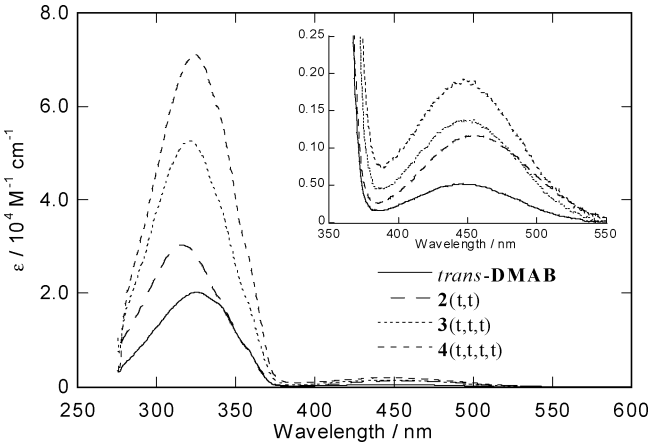

FIGURE 6. Absorption spectra of *trans*-**DMAB**, **2**(t,t), **3**(t,t,t), and **4**(t,t,t,t) in benzene.

TABLE 2. Absorption Maxima (λ_{max}) and Molar Extinction Coefficients (ϵ) of Macrocycles in Benzene

compd	λ_{max}/nm (ϵ/M^{-1} cm^{-1})
trans-DMAB	325 (20130), 445 (518)
2(t,t)	316 (30300), 455 (1170)
3(t,t,t)	321 (52600), 450 (1350)
4(t,t,t,t)	324 (71200), 447 (1930)

molecule. This result is in contrast to the crystal of **3**(t,t,t), where the benzene rings faced the solvent molecule. In a single channel, the chlorine atoms of dichloromethane molecules were located in a straight line. The distance between the dichloromethane molecules was 6.39 Å.

Absorption Spectra. The absorption spectra of all-trans isomers of **2**−**4** are shown in Figure 6, and the molar extinction coefficients are listed in Table 2 together with the data for *trans*-3,3′-dimethylazobenzene (*trans*-**DMAB**). As was expected, the value of ϵ was increased as the number of azobenzene units increased. However, both ϵ and λ_{max} of **2**(t,t) were shifted compared to those of other compounds. In the $S_1(n,\pi^*)$ band, ϵ of **2**(t,t) was larger than twice the value for *trans*-**DMAB**, while ϵ of the $S_2(\pi,\pi^*)$ band of **2**(t,t) was smaller than twice the value for *trans*-**DMAB**. The absorption maximum (λ_{max}) of **2**(t,t) was shifted by 10 nm to a longer wavelength in the $S_1(n,\pi^*)$ band, and by 9 nm to a shorter wavelength in the $S_2(\pi,\pi^*)$ band compared to those for *trans*-**DMAB**. As the ring size was enlarged, λ_{max} of both the $S_1(n,\pi^*)$ and $S_2(\pi,\pi^*)$ bands shifted in the opposite direction. In the $S_1(n,\pi^*)$ band, λ_{max} shifts to longer wavelength as the ring size increases. On the other hand, λ_{max} shifts to a shorter wavelength in the $S_2(\pi,\pi^*)$ band. The λ_{max} of **4**(t,t,t,t) was very close to that of *trans*-**DMAB**. These spectrum shifts are dependent on the ring size and might originate from the steric distortion of the azobenzene units.

Thermal Isomerization of 2. Thermal cis-to-trans isomerization reactions which proceeded stepwise from **2**(c,c) to **2**(t,c) and from **2**(t,c) to **2**(t,t) were observed. The lifetimes (1/k) of **2**(c,c) and **2**(t,c) at 298 K in acetonitrile were 19.7 days ($k_1 = 5.87 \times 10^{-7}$ s^{-1}) and 6.1 days ($k_2 = 1.89 \times 10^{-6}$ s^{-1}), respectively. The lifetimes of both isomers were longer than that of *cis*-azobenzene (4.7 days).[13] Thermodynamic parameters of each process were determined by the Eyring equation[14] by measuring the first-order rate constants at different temperatures. In the isomerization process of **2**(c,c) to **2**(t,c), $\Delta H^{\ddagger} = 22.6$ kcal mol^{-1} and $\Delta S^{\ddagger} = -11.4$ cal K^{-1} mol^{-1} were obtained. On the other hand, in the isomerization process of **2**(t,c) to **2**(t,t), the values were $\Delta H^{\ddagger} = 25.0$ kcal mol^{-1} and $\Delta S^{\ddagger} = -0.6$ cal K^{-1} mol^{-1}. Despite the fact that the $\Delta H^{\ddagger}$ value of the former process is lower than that of the latter process, the lifetime of **2**(c,c) (19.7 days) is about three times that of **2**(t,c) (6.1 days) at room temperature.

Photochemical Isomerization of 2. As described above, **2**(t,t) isomerized to give **2**(t,c), followed by the isomerization to **2**(c,c) upon photoirradiation. A plot of the isomer ratio of **2** vs irradiation time upon 313-nm irradiation is shown in Figure 7a. In the beginning, a rapid decrease in **2**(t,t) and an increase in **2**(t,c) were observed. **2**(t,c) reached the maximum in about 32 min, and the ratio at that time is about 48%. The ratio of **2**(c,c) rose after **2**(t,c), and the ratio of all isomers became constant after 150 min (photostationary state). The isomer ratio at the photostationary state on 313-nm irradiation was 0.14, 0.29, and 0.57 for **2**(t,t), **2**(t,c), and **2**(c,c), respectively. Table 3 shows the isomer ratio at the photostationary state at various excitation wavelengths. At the 366-nm photostationary state, the isomer ratio was 0.02, 0.11, and 0.87 for **2**(t,t), **2**(t,c), and **2**(c,c), respectively. This mixture at the 366-nm photostationary state was further irradiated at 436 nm, and the ratio of the isomers was monitored as shown in Figure 7b. The ratio of **2**(c,c) dropped as **2**(t,c) increased. The ratio of **2**(t,c) hit the maximum (60%) at $t = 25$ min. The ratio of **2**(t,t) increased on prolonged irradiation, and the photostationary state was established after 80 min (**2**(t,t):**2**(t,c):**2**(c,c) = 0.45:0.49:0.06).

To estimate the steric effect on the photoisomerization of **2**, the quantum yields for all the isomerization steps

(13) Asano, T.; Okada, T.; Shinkai, S.; Shigematsu, K.; Kusano, Y.; Manabe, O. *J. Am. Chem. Soc.* **1981**, *103*, 5161−5165.
(14) Eyring, H. *Chem. Rev.* **1935**, *17*, 65−77.

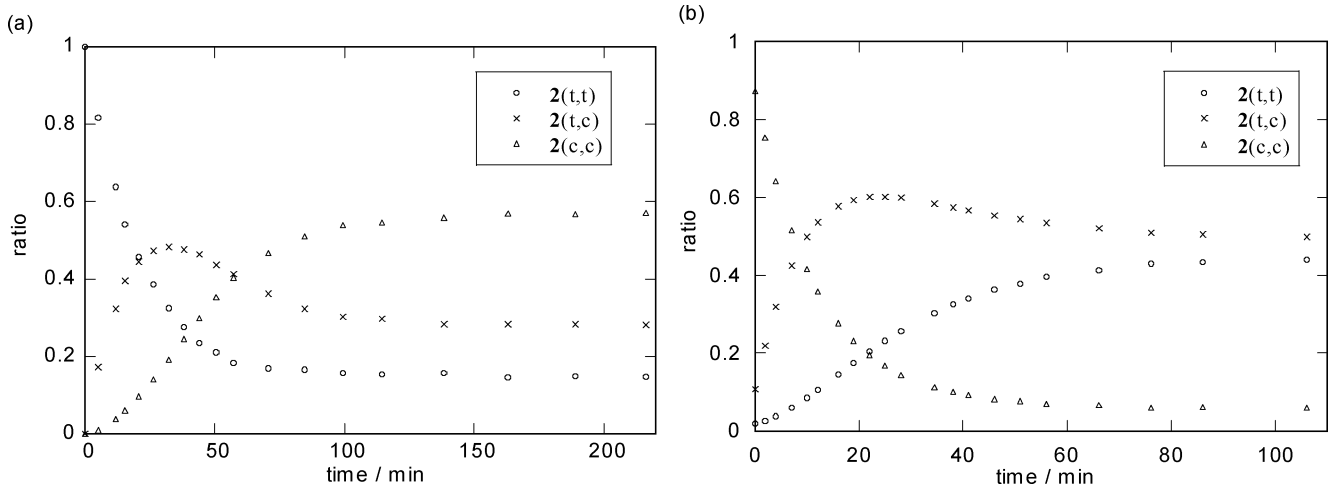

FIGURE 7. Relative concentration of isomers of **2** vs irradiation time on photoirradiation at 313 nm (a) and at 436 nm after the establishment of the 366-nm photostationary state (b) in acetonitrile. The initial concentration of **2**(t,t) was 1.15×10^{-4} M.

TABLE 3. Isomer Ratio at the Photostationary State of 2 at Various Irradiation Wavelengths in Acetonitrile

irradiation wavelength/nm	**2**(t,t)	**2**(t,c)	**2**(c,c)
313	0.14	0.29	0.57
366	0.02	0.11	0.87
436	0.45	0.49	0.06

TABLE 4. Quantum Yields of Isomerization of 2 on Excitation at 313 and 436 nm in Acetonitrile

irradiation wavelength/nm	Φ_{tt-tc}	Φ_{tc-tt}	Φ_{tc-cc}	Φ_{cc-tc}
313	0.25	0.26	0.09	0.18
436	0.34	0.35	0.15	0.51

were determined upon 313- and 436-nm excitation. The procedure is explained in the Experimental Section, and the obtained quantum yields are listed in Table 4. The quantum yields are defined by using the ratio of photons leading to isomerization/absorbed photons by the molecule as a whole. Upon 313-nm irradiation, Φ_{tt-tc} (0.25) was three times Φ_{tc-cc} (0.09), although both processes involve the isomerization of trans-to-cis direction. As for the cis-to-trans isomerization, Φ_{tc-tt} (0.26) was larger than Φ_{cc-tc} (0.18). The quantum yields of the isomerization between **2**(t,t) and **2**(t,c) were higher than those between **2**(t,c) and **2**(c,c). Upon 436-nm irradiation, Φ_{tt-tc} (0.34) was larger than Φ_{tc-cc} (0.15), with a tendency similar to that of the 313-nm excitation. However, Φ_{tc-tt} (0.35) was smaller than Φ_{cc-tc} (0.51), with a tendency opposite to that of the 313-nm irradiation. Dependence on the excitation wavelength of the quantum yields was observed. The value of Φ_{tt-tc} was different on 313- and 436-nm irradiation, and the difference was beyond experimental error. The value of Φ_{cc-tc} has the largest dependence: the efficiency is about three times higher on 436-nm excitation than on 313-nm excitation.

Photochemical Isomerization of 3 and 4. Both **3** and **4** exhibited stepwise isomerization upon photoirradiation, and all the isomers could be observed by HPLC. The ratios of the isomers of **3** and **4** at the photostationary state on the excitation at 366 and 436 nm are listed in Tables 5 and 6, respectively. There are four isomers in **3**

TABLE 5. Isomer Ratio at the Photostationary State of 3 at Various Irradiation Wavelengths in Chloroform

irradiation wavelength/nm	**3**(t,t,t)	**3**(t,t,c)	**3**(t,c,c)	**3**(c,c,c)
366	0.02	0.07	0.27	0.64
436	0.51	0.38	0.10	0.01

TABLE 6. Isomer Ratio at the Photostationary State of 4 at Various Irradiation Wavelengths in Chloroform

irradiation wavelength/nm	**4**(t,t,t,t)	**4**(t,t,t,c)	**4**(t,t,c,c)	**4**(t,c,t,c)	**4**(t,c,c,c)	**4**(c,c,c,c)
366	0.004	0.022	0.061	0.030	0.27	0.61
436	0.40	0.42	0.10	0.055	0.024	0.002

[**3**(t,t,t), **3**(t,t,c), **3**(t,c,c), and **3**(c,c,c)], while six isomers exist in **4** [**4**(t,t,t,t), **4**(t,t,t,c), **4**(t,t,c,c), **4**(t,c,t,c), **4**(t,c,c,c), and **4**(c,c,c,c)]. In both compounds, the number of *cis*-azobenzene units increased upon irradiation at 366 nm and decreased at 436-nm irradiation. Both **4**(t,t,c,c) and **4**(t,c,t,c) consist of two *trans*-azobenzene and two *cis*-azobenzene units, but the position of these azobenzene units is different. The azobenzene units with the same configuration are next to each other in **4**(t,t,c,c), but are on the opposite side of the ring in **4**(t,c,t,c). These two isomers could be observed by HPLC and their ratio was always ca. 2:1, regardless of the excitation wavelength. The ratio of **4**(t,t,c,c) is always twice that of **4**(t,c,t,c) because the trans-to-cis isomerization from **4**(t,t,t,c) takes place with the ratio of probability of 2:1 for **4**(t,t,c,c) and **4**(t,c,t,c). When a *trans*-azobenzene unit in **4**(t,t,t,c) isomerizes to cis, there are three possible ways to choose one *trans*-azobenzene unit. Two *trans*-azobenzene units are next to the *cis*-azobenzene unit in **4**(t,t,t,c), and the trans-to-cis isomerization of these *trans*-azobenzene units results in the formation of **4**(t,t,c,c). On the other hand, **4**(t,c,t,c) is formed by the trans-to-cis isomerization of the *trans*-azobenzene unit, which is on the opposite side of the *cis*-azobenzene unit in **4**(t,t,t,c). The same argument can be applied to the cis-to-trans isomerization from **4**(t,c,c,c). Thus, the ratio of the concentration of **4**(t,t,c,c) and **4**(t,c,t,c) is always 2:1, assuming that the probability of the isomerization does not depend on the position in the ring.

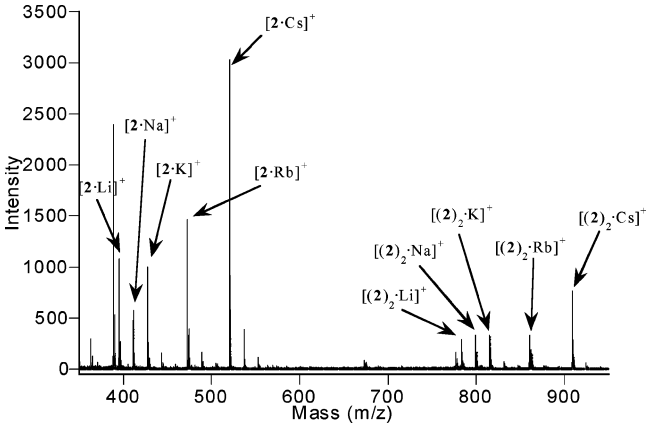

FIGURE 8. ESI mass spectrum of dimer **2**(t,t) binding M^+ (Li^+, Na^+, K^+, Rb^+, and Cs^+). [**2**] = 0.25 mM, [M^+] = 0.25 mM.

Complexation with Alkaline Metal Cations. The property of the macrocyclic azobenzenes as the host for alkaline metal cations (Li^+, Na^+, K^+, Rb^+, Cs^+) was evaluated by electrospray ionization mass spectrometry (ESIMS). Herein we show the preliminary results, and we discuss the possibility of controlling the ion selectivity by light irradiation in a later section.

A methanol solution that contained an equal concentration of **2**(t,t) and a mixture of the alkaline metal cations was subjected to the measurement by ESIMS and the spectra were obtained as shown in Figure 8. The 1:1 complex consists of **2**(t,t) and a metal cation ([**2**·M]$^+$) was observed, and its relative selectivity was highest for ([**2**·Cs]$^+$). Moreover, the 2:1 complex, which consists of two molecules of **2**(t,t) and a metal cation ([(**2**)$_2$·M]$^+$), was also observed, with the highest selectivity for [(**2**)$_2$·Cs]$^+$. The mass spectra of the methanol solution of *trans*-3,3′-dimethylazobenzene (*trans*-**DMAB**) and these alkali metal cations were measured. The observed spectra consist of the major signal of [**DMAB**·H]$^+$, minor signals attributed to the 1:1 complexes ([**DMAB**·M]$^+$), and no signal for the 2:1 complexes. No substantial change was observed in the spectra on photoirradiation of *trans*-**DMAB**.

To study the change in the ion selectivity upon photoisomerization, a solution of **2**(t,t) was irradiated at 366 or 436 nm to the photostationary state, prior to mixing with the metal ion solution. The relative intensities of the mass spectra of each of the complexes with or without photoirradiation are shown in Figure 9. In the 1:1 complex, the relative selectivity of Li^+ decreased and that of Na^+ increased upon irradiation at either wavelength. However, the change was small and the selectivity of larger metal cations was unchanged. In the 2:1 complex, on the other hand, the relative intensity of the Cs^+ complex was the largest without photoirradiation, but it decreased upon photoirradiation. The relative intensity of the complex with Li^+ ([(**2**)$_2$·Li]$^+$) increased when the molar fraction of **2**(t,c) was high (∼50% at 436-nm irradiation). Upon 366-nm irradiation, as the ratio of **2**(c,c) increased, [(**2**)$_2$·Na]$^+$ and [(**2**)$_2$·K]$^+$ had higher intensity.

The ESIMS spectrum was observed on the mixture of the same concentrations of **3**(t,t,t) and alkaline metal cations (Li^+, Na^+, K^+, Rb^+, Cs^+). Similar to the spectra of **2**(t,t), two types of complexes, [**3**·M]$^+$ and [(**3**)$_2$·M]$^+$, were observed. The selectivity for Cs^+ was the highest in both the 1:1 and 2:1 complexes irrespective of the photoirradiation (Figure 10). In the 1:1 complex, the spectra did not exhibit a substantial change upon photoirradiation at either 436- or 366-nm irradiation. As for the 2:1 complex, however, the relative intensity of [(**3**)$_2$·Na]$^+$ and [(**3**)$_2$·K]$^+$ was higher as well as that of [(**3**)$_2$·Cs]$^+$ without irradiation, while [(**3**)$_2$·Na]$^+$ and [(**3**)$_2$·K]$^+$ were increased and [(**3**)$_2$·Cs]$^+$ was decreased upon 436-nm irradiation (**3**(t,t,t):**3**(t,t,c):**3**(t,c,c):**3**(c,c,c) = 51:38:10:1). At the photostationary state of 366-nm irradiation (**3**(t,t,t):**3**(t,t,c):**3**(t,c,c):**3**(c,c,c) = 2:7:27:64), the obtained spectrum was similar to that without irradiation.

The most remarkable effect on the ratio of the complexes was observed upon the photoirradiation of **4**(t,t,t,t). The ESIMS spectrum observed for the mixture of the same concentrations of **4**(t,t,t,t) and alkaline metal cations (Li^+, Na^+, K^+, Rb^+, Cs^+) was also similar to that of **2** and **3**. The 1:1 and 2:1 complexes were observed. In the 1:1 complex, the intensity was highest at [**4**·Cs]$^+$, in analogy with **2**(t,t) and **3**(t,t,t). On photoirradiation, however, the decrease in the intensity of [**4**·Cs]$^+$ was observed accompanied by the increase in the complexes with smaller metal cations (Li^+ and Na^+), as the number of *cis*-azobenzene units was increased (Figure 11). A similar effect was observed for the 2:1 complex upon photoirradiation.

Discussion

Structure of Azobenzenophanes. To estimate the effect of the ring size on the structure of the macrocycles, the structures of the *trans*-azobenzene units of each of the macrocycles are compared in Figure 12. Their bond and dihedral angles are listed in Table 1 along with the reported values for *trans*- and *cis*-azobenzene. Arrows designated as a and b in Figure 12 indicate the view from which the azobenzene unit is seen. The *trans*-azobenzene unit loses its planarity with decreasing ring size. The torsion angles of the C−N═N−C bond are twisted ca. 10° from the planar structure in **2**(t,t) and **2**(t,c), while they are almost planar in **3**(t,t,t) and **4**(t,t,t,t). In the torsion angles of N═N−C═C, **2**(t,t) and **3**(t,t,t) are similar, and these values are close to that of *trans*-azobenzene, while **4**(t,t,t,t) exhibits smaller values. In **2**(t,c), one benzene ring is tilted about 25° versus the N═N−C plane in both conformers C and D. In the bond angles of N═N−C, the two values in a single azobenzene unit are almost equal for both **3**(t,t,t) and **4**(t,t,t,t), whereas they are varied in **2**(t,t) and **2**(t,c). For example, the N═N−C bond angles are very close: 106 and 105° in **3**(t,t,t), but 113 and 103° in **2**(t,t). The broken arrows in Figure 12 indicate the distance between the carbon atoms of the methylene linkers. In **2**(t,t) and **2**(t,c), the distances are 8.39 and 8.24 Å, respectively. These values are smaller than those in **3**(t,t,t) and **4**(t,t,t,t), which are 9.25 and 9.13 Å, respectively. The distance calculated by the AM1 semiempirical calculation was 9.30 Å in *trans*-**DMAB**. Therefore, these facts indicate that the *trans*-azobenzene units in **2**(t,t) and **2**(t,c) are bent toward the inside of the cavity, and the ring strains of **3**(t,t,t) and **4**(t,t,t,t) are relatively small.

The structure of the *cis*-azobenzene units of **2**(t,c) and **2**(c,c) are shown in Figure 13, and the torsion and the bond angles are listed in Table 1, along with the reported

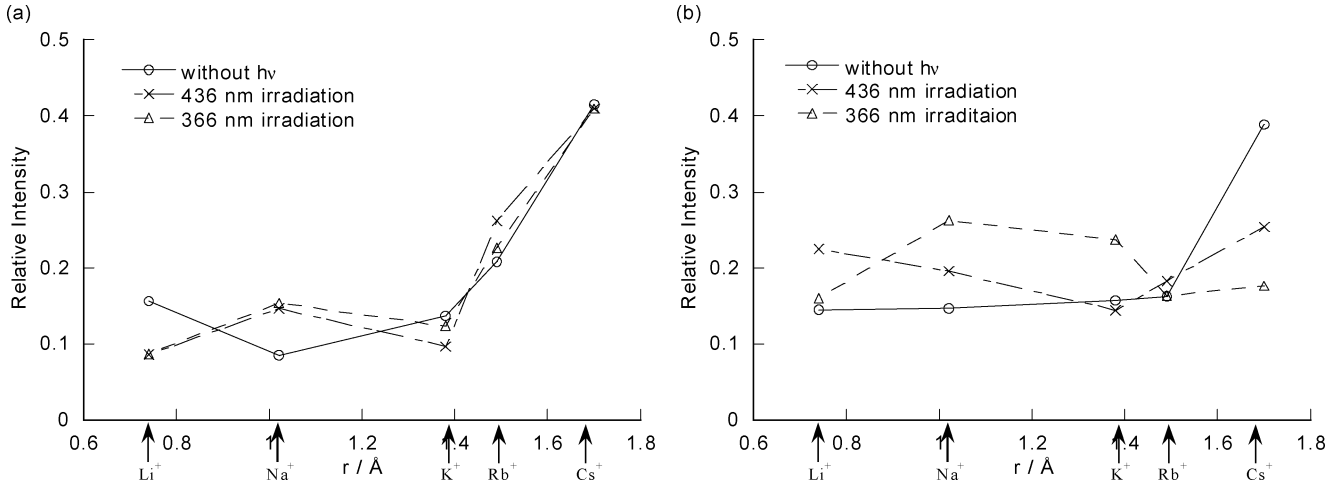

FIGURE 9. Plots of relative intensity of ESI mass spectra of **2** vs metal ion radius for 1:1 (a) and 2:1 (b) dimer−ion complexes. Samples were prepared in the dark or irradiated at 436 or 366 nm before the dimer solution was mixed with the metal ion solution.

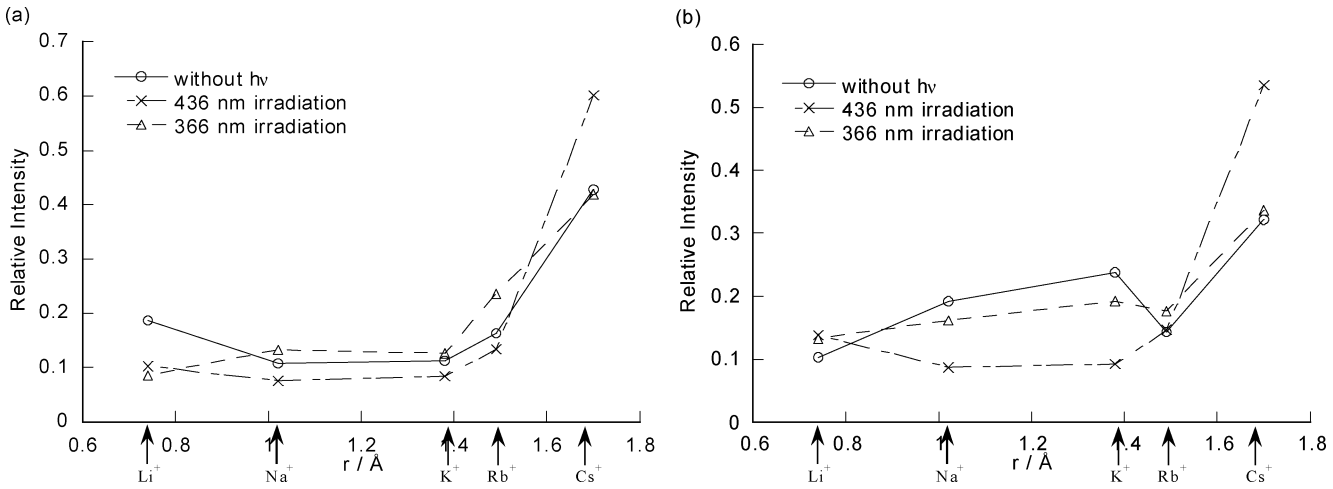

FIGURE 10. Plots of relative intensity of ESI mass spectra of **3** vs metal ion radius for 1:1 (a) and 2:1 (b) trimer−ion complexes. Samples were prepared in the dark or irradiated at 436 or 366 nm before the trimer solution was mixed with the metal ion solution.

values for *cis*-azobenzene. In **2**(t,c), the C−N═N−C bond is twisted only 1° from the planar cis configuration. However, the dihedral angles of the N═N−C═C bond are −51 and −91°, indicating that one benzene ring is perpendicular to the N═N−C plane. The bond angles of the N═N−C bond showed that the *cis*-azobenzene unit is bent to the outside of the cavity. In contrast, the ring strain in **2**(c,c) is very small. The structure of the *cis*-azobenzene unit of **2**(c,c) is very close to that of *cis*-azobenzene[12] as shown in Table 1.

From the above discussions, the magnitude of the ring strain is largest in **2**(t,c) and the next largest is **2**(t,t). The ring strains in **3**(t,t,t) and **4**(t,t,t,t) are very small.

Effect of Steric Distortion on Absorption Spectra. The X-ray crystal analyses have revealed that the *trans*-azobenzene unit of **2**(t,t), which is the chromophore of the compound, has a distorted structure and loses its planarity in the crystal phase. In solution, one might expect that the **2**(t,t) has a structure similar to that in the crystal phase, and the π-resonance of the chromophore is different from that of *trans*-azobenzene to some extent. Actually, the observed peak shift and the change in the peak intensity in the absorption spectra can be explained by the ring strain. The absorption maxima (λ_{max}) are 455 and 316 nm in **2**(t,t), but are 445 and 325 nm in *trans*-**DMAB**. The $S_1(n,\pi^*)$ band was red-shifted and the $S_2(\pi,\pi^*)$ band was blue-shifted by the cyclic structure. A shift of the λ_{max} was also observed in **3**(t,t,t) and **4**(t,t,t,t); however, the shift was dependent on the ring size. The shift became smaller as the ring size increased. Comparing the molar extinction coefficient at λ_{max} per azobenzene unit, ϵ = 500 and 575 M^{-1} cm^{-1} in the $S_1(n,\pi^*)$ band, while ϵ = 19 900 and 16 900 M^{-1} cm^{-1} in the $S_2(\pi,\pi^*)$ band for *trans*-**DMAB** and **2**(t,t), respectively. Thus, the n,π^* band has been enhanced, and the π,π^* band has been weakened by the cyclic structure. These observations can be elucidated qualitatively by the overlap of orbitals in the *trans*-azobenzene unit, in which the steric distortion results in an increase in the overlap between n and π^* orbitals and a decrease in that between π and π^* orbitals.

Effect of Steric Distortion on Thermal Isomerization of 2. In the two thermal isomerization processes, **2**(c,c)-to-**2**(t,c) and **2**(t,c)-to-**2**(t,t), the former process is

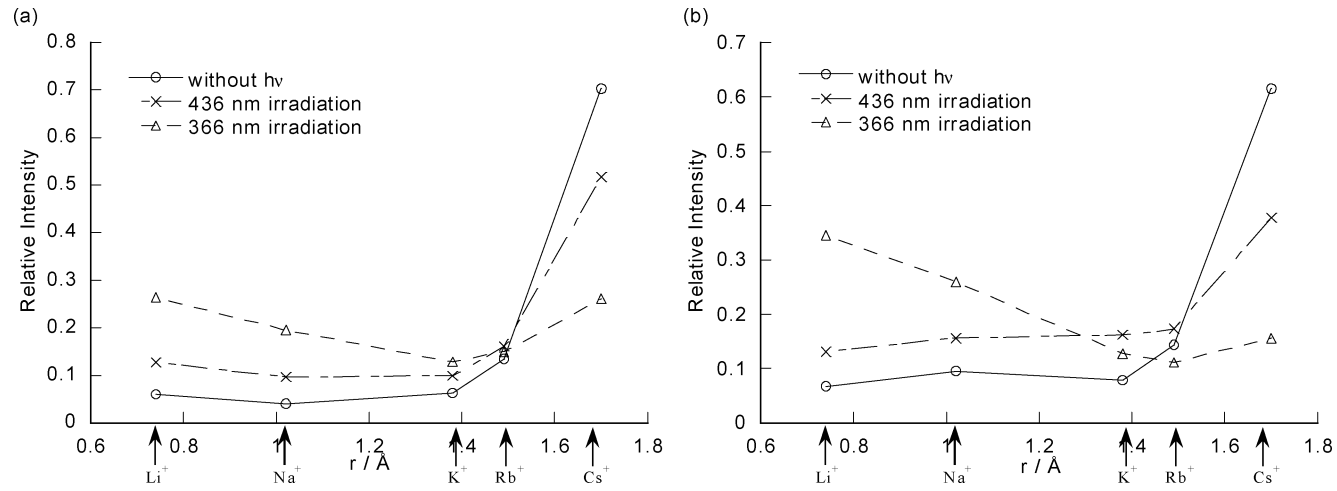

FIGURE 11. Plots of relative intensity of ESI mass spectra of **4** vs metal ion radius for 1:1 (a) and 2:1 (b) tetramer−ion complexes. Samples were prepared in the dark or irradiated at 436 or 366 nm before the tetramer solution was mixed with the metal ion solution.

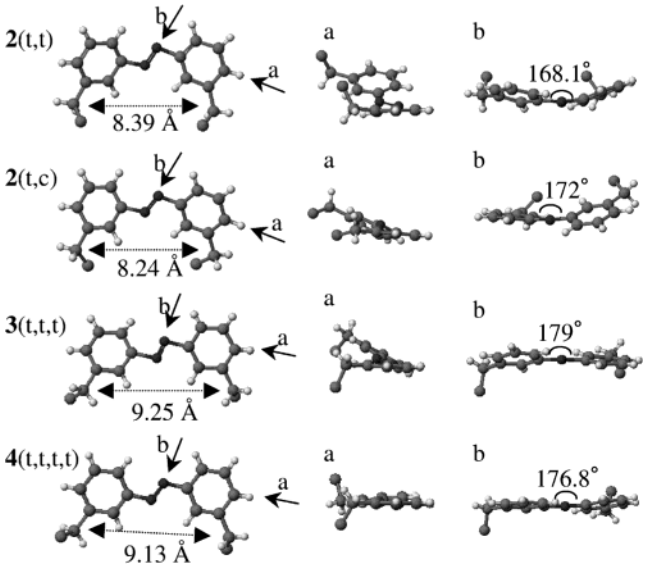

FIGURE 12. *trans*-Azobenzene units of **2**(t,t), **2**(t,c), **3**(t,t,t), and **4**(t,t,t,t).

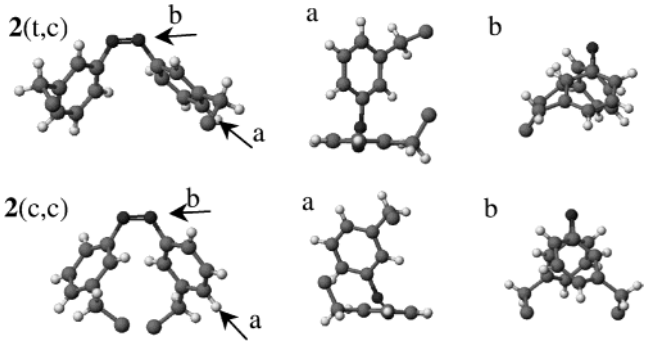

FIGURE 13. *cis*-Azobenzene units of **2**(t,c) and **2**(c,c).

approximately three times slower than the latter process, despite having the former $\Delta H^{\ddagger}$ value that is 2.4 kcal mol^{-1} lower than the latter. The $\Delta S^{\ddagger}$ values are −11.4 and −0.6 cal K^{-1} mol^{-1} for the former and the latter processes, respectively. Thus, the main factor that governs the isomerization rate is the $\Delta S^{\ddagger}$ value, because it reflects the difference in the degree of freedom between the ground and the transition states. There might be two reasons for the relatively small value of $\Delta S^{\ddagger}$ in the former process. First, the transition state in the thermal isomerization from **2**(c,c) to **2**(t,c) has a sterically unfavorable structure that has a lower degree of freedom than the transition state between **2**(t,c) and **2**(t,t). The structure of the transition state and the reaction pathway should be revealed to discuss this point. Second, the isomerization of **2**(t,c) starts from a structure that has a smaller degree of freedom because of the strain due to the cyclic structure. The structures from which the thermal isomerization starts are deducible by the X-ray crystal structures, where the *cis*-azobenzene unit in **2**(t,c) has more ring strain than that of **2**(c,c).

To evaluate the relative stability among the three isomers, the heats of formation were estimated by ab initio quantum chemical calculations. We employed the RHF/6-31G** method.[15] The molecular structures, which were obtained by the X-ray crystal structure analyses, were used for the initial structure and the geometries were fully optimized. The obtained structures are shown in Figure 14 and the selected bond angle and torsion angles are listed in Table 1. The results show that **2**(t,t) is 14 kcal mol^{-1} more stable than **2**(t,c), and **2**(t,c) is 7.7 kcal mol^{-1} more stable than **2**(c,c). A HF/6-31+G* study showed that *trans*-azobenzene is about 18 kcal mol^{-1} more stable than *cis*-azobenzene.[16] An experimental study on the heat of combustion of *trans*- and *cis*-azobenzene indicated that *trans*-azobenzene is about 10

(15) Frisch, M. J.; Trucks, G. W.; Schlegel, H. B.; Scuseria, G. E.; Robb, M. A.; Cheeseman, J. R.; Zakrzewski, V. G.; Montgomery, J. A., Jr.; Stratmann, R. E.; Burant, J. C.; Dapprich, S.; Millam, J. M.; Daniels, A. D.; Kudin, K. N.; Strain, M. C.; Farkas, O.; Tomasi, J.; Barone, V.; Cossi, M.; Cammi, R.; Mennucci, B.; Pomelli, C.; Adamo, C.; Clifford, S.; Ochterski, J.; Petersson, G. A.; Ayala, P. Y.; Cui, Q.; Morokuma, K.; Malick, D. K.; Rabuck, A. D.; Raghavachari, K.; Foresman, J. B.; Cioslowski, J.; Ortiz, J. V.; Baboul, A. G.; Stefanov, B. B.; Liu, G.; Liashenko, A.; Piskorz, P.; Komaromi, I.; Gomperts, R.; Martin, R. L.; Fox, D. J.; Keith, T.; Al-Laham, M. A.; Peng, C. Y.; Nanayakkara, A.; Challacombe, M.; Gill, P. M. W.; Johnson, B.; Chen, W.; Wong, M. W.; Andres, J. L.; Gonzalez, C.; Head-Gordon, M.; Replogle, E. S.; Pople, J. A. *Gaussian 98*, Revision A.9; Gaussian, Inc.: Pittsburgh, PA, 1998.

(16) Kurita, N.; Tanaka, S.; Itoh, S. *J. Phys. Chem. A* **2000**, *104*, 8114−8120.

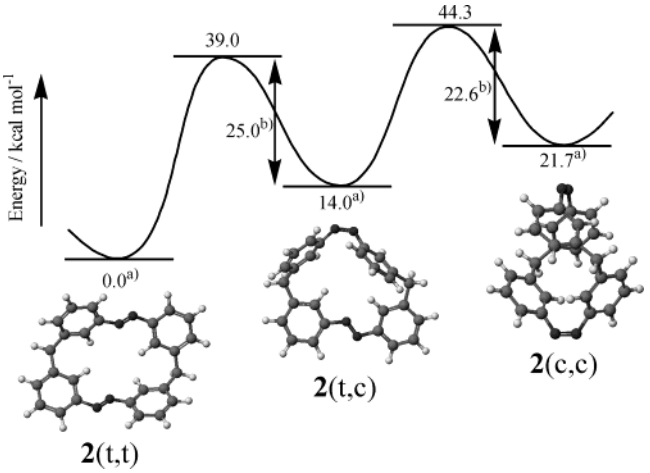

FIGURE 14. Energy diagram of **2** estimated from the experiment and the theoretical calculations. Structures shown were obtained by RHF/6-31G** calculations: (a) calculated by RHF/6-31G** and (b) experimental values.

kcal mol^{-1} more stable than *cis*-azobenzene.[17] The relatively small energy difference between **2**(t,c) and **2**(c,c) (7.7 kcal mol^{-1}) indicates that **2**(t,c) is destabilized by the ring strain. One might expect that **2**(t,t) is also destabilized; however, the energy difference between **2**(t,t) and **2**(t,c) (14.0 kcal mol^{-1}) is almost twice that between **2**(t,c) and **2**(c,c). Thus, from the quantum chemical calculations, the steric distortion is largest in **2**(t,c). An energy diagram depicted from the experimental and theoretical results is shown in Figure 14. The diagram shows that the ring strain destabilizes both **2**(t,c) and the transition state between **2**(t,c) and **2**(t,t). The effect of the ring strain results in the relatively higher value of $\Delta H^{\ddagger}$ in **2**(t,c) to **2**(t,t); however, the reaction rate is still faster because of the effect of the entropy ($\Delta S^{\ddagger}$).

Several studies on the cyclic azobenzene dimers, consisting of two or three atomic chains, indicate that the stability of cis isomers is dependent on the chain length and the position where the chain is connected. Rau et al. reported that azobenzenophane, in which two azobenzenes are connected by $-CH_2-S-CH_2-$ chains at the para positions (**1a**), exhibited a lifetime of 6.25 min for the t,c isomer, while that of ca. 5 days for the c,c isomer at 298 K.[6a] Tamaoki et al. reported that the lifetime of the t,c isomer was even shorter (22 s) in azobenzenophane, with $-CH_2-CH_2-$ chains at the para positions (**1b**), while the lifetime of the c,c isomer was ca. 2.5 days.[6b,c] The shortest lifetime of the t,c isomer was observed in azobenzenophane, in which two azobenzenes are connected by benzene rings. Its t,c isomer had a lifetime of 1.3 s, while that of the c,c isomer was 3.2 h.[6d] In these compounds, the lifetimes of both trans,cis and cis,cis isomers strongly depend on the length of the chains. The lifetimes of the trans,cis isomers are much shorter than those of the cis,cis isomers. It seems that the *cis*-azobenzene unit in the trans,cis form is forced toward the outside of the molecular cavity. In contrast, *o*-azobenzenophane, in which two azobenzenes are connected at the ortho positions by $-CH_2-CH_2-$ chains, shows different behavior in that the lifetime of the t,c isomer (ca. 6 weeks) is longer than that of the c,c isomer (ca. 6 days).[6h] It seems that the *cis*-azobenzene unit in the trans,cis isomer is stabilized by the force toward the inside of the cavity because the carbon chains on the *cis*-azobenzene unit are fixed close to each other by the connection with the *trans*-azobenzene unit on the ortho positions. As for the *m*-azobenzenophane, the ring strain on the trans,cis isomer is intermediate between that of the *p*- and *o*-azobenzenophanes. The lifetime of **2**(t,c) (6.1 days) is between them, though the chain length is the shortest. Although the X-ray crystal structure analysis revealed that the benzene rings are forced toward the outside of the cavity, the ring strain is relatively small compared to that of the para-substituted azobenzenophanes. Thus, the stability of the trans,cis isomers of azobenzenophanes depends strongly on the position of the linkers as well as on the chain length. In cis,cis isomers, on the other hand, the lifetime is not as dependent on the structure of azobenzenophanes (2−20 days) as is that of the trans,cis isomers (seconds to 6 weeks).[6a−h] Steric distortion seems to be relatively small because the two azobenzene units in a single molecule have the same cis geometry, and the positions where the linkers are connected in each azobenzene unit are close to each other; the linkers can reach from one azobenzene unit to the other without causing substantial steric hindrance regardless of the position or the length of the linkers.

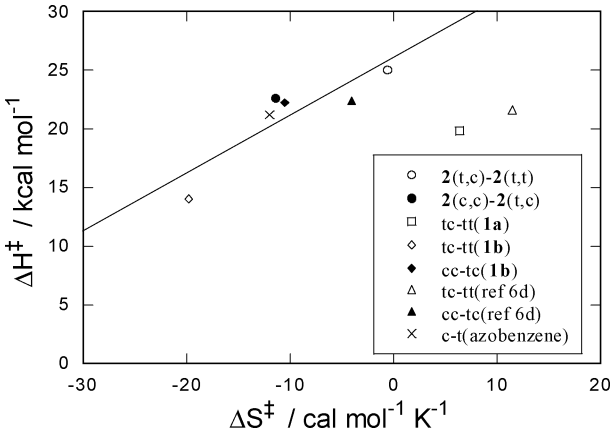

FIGURE 15. Isokinetic plot for $\Delta H^{\ddagger}$ and $\Delta S^{\ddagger}$ of the cis−trans thermal isomerization of cyclic azobenzene dimers. Square, cited from ref 6a. Diamonds, cited from ref 6b,c. Triangles, cited from ref 6d. Cross, cited from ref 13.

A linear $\Delta H^{\ddagger}-\Delta S^{\ddagger}$ relationship has often been used as an indication for discussing the reaction mechanism of the thermal cis−trans isomerization of azobenzene and related compounds.[13,18,19,20] $\Delta H^{\ddagger}$ tends to increase with an increase in $\Delta S^{\ddagger}$. The relationship is called an isokinetic or compensation relationship. This relation holds when the reaction occurs via a single mechanism.[13] Figure 15 shows the isokinetic plot of a series of cyclic azobenzene dimers for which the thermodynamic parameters ($\Delta H^{\ddagger}$ and $\Delta S^{\ddagger}$) have been reported. Those values of azobenzene[13] are also plotted. The plot can be fitted by a straight

(17) Corruccini, R. J.; Gilbert, E. C. *J. Am. Chem. Soc.* **1939**, *61*, 2925−2927.

(18) Nishimura, N.; Sueyoshi, T.; Yamanaka, H.; Imai, E.; Yamamoto, S.; Hasegawa, S. *Bull. Chem. Soc. Jpn.* **1976**, *49*, 1381−1387.

(19) Otruba, J. P., III; Weiss, R. G. *J. Org. Chem.* **1983**, *48*, 3448−3453.

(20) Kuriyama Y.; Oishi, S. *Chem. Lett.* **1999**, 1045−1046.

line except for the two points which correspond to the trans,cis−trans,trans processes in **1a** and the compound reported in ref 6d. The straight line corresponds to the line for various noncyclic azobenzenes that has been reported and assigned to the inversion mechanism.[13,19,20] Thus, the inversion mechanism might be operative in the thermal isomerization processes which exhibit the compensation relationship. The steric distortion by the cyclic structure does not alter the isomerization mechanism but changes the degree of freedom and the stability of the transition state. Last, we should mention the two points far from the fitted line in Figure 15. Both processes involve the trans,cis to trans,trans isomerization of *p*-azobenzenophanes. The steric distortion of the trans,cis isomer of the *p*-azobenzenophane is very large. Thus, the structure of the starting point (trans,cis geometry) for the thermal isomerization might be different from the other azobenzenophanes, although the reaction proceeds via the common transition state geometry.

Effect of Steric Distortion on Photochemical Isomerization of 2. (a) 313-nm Excitation. The quantum yields for the isomerization of **2**(t,t)-to-**2**(t,c) ($\Phi_{tt-tc} = 0.25$) and **2**(t,c)-to-**2**(c,c) ($\Phi_{tc-cc} = 0.09$) were different, although both processes are in the trans-to-cis direction. In the isomerization of **2**(t,t)-to-**2**(t,c), the absorption of a photon takes place at either azobenzene unit in a single molecule and results in the formation of the same product (**2**(t,c)) with equal probabilities. On the other hand, two kinds of azobenzene units, trans and cis configurations, exist in **2**(t,c). Thus, either *trans*- or *cis*-azobenzene units can absorb a photon on the irradiation of **2**(t,c). When **2**(t,c) is excited at 313 nm, about 95% of the photons are expected to be absorbed by the *trans*-azobenzene unit, because the molar extinction coefficients (ϵ) of *trans*- and *cis*-azobenzene are $\epsilon = 21\,100$ and $1\,160$ M^{-1} cm^{-1}, respectively.[21] Nevertheless, Φ_{tc-cc} is relatively low for the trans-to-cis isomerization of azobenzene and is even lower than the quantum yield for the isomerization of **2**(t,c)-to-**2**(t,t) ($\Phi_{tc-tt} = 0.26$) despite the small probability of the absorption of a photon for the *cis*-azobenzene unit. These facts can be explained by the following assumptions. First, the transition state between **2**(t,c) and **2**(c,c) in the excited state (either the S_1 or S_2 state) has a smaller degree of freedom due to the steric distortion. Generally, the deactivation to the ground state takes place at the midpoint (either the N−N−C atoms are aligned in a line in the "inversion" mechanism or the dihedral angle of the C−N−N−C bond is 90° in the "rotation" mechanism) between the trans and cis isomers of azobenzene. In either mechanism, the structure of the transition state has ring strain to some extent. As a consequence of the distorted structure of the transition state, the structural change is inhibited and the deactivation from the **2**(t,c) side is enhanced. Second, the energy transfer from the *trans*- to the *cis*-azobenzene units might occur, and it would give a higher Φ_{tc-tt} value. As described above, nearly 95% of the photons are expected to be absorbed by the *trans*-azobenzene unit. However, the Φ_{tc-tt} exceeded the ratio of the photons absorbed by the *cis*-azobenzene unit (∼5%). If the energy transfer does not take place, the Φ_{tc-tt} stays below 0.05, because the formation of **2**(t,t) requires the excitation of the *cis*-azobenzene unit in **2**(t,c). Thus, the value indicates the possibility of the energy transfer where the excitation energy of the *trans*-azobenzene unit is transferred to the *cis*-azobenzene units. From the above discussion, it should be noted that there are intramolecular interactions between azobenzene chromophores, such as steric distortion and energy transfer between the chromophores in **2**. To our knowledge, energy transfer in azobenzenes in solution has not been reported, because of their short excited-state lifetime.[9] The comparison with the noncyclic analogue will be valid to support this conclusion. Recently, it has been reported that the cis/trans isomer ratio of azobenzene at the photostationary state was dependent on the concentration. The mechanism for the effect has been explained by the formation of a dimer biradical singlet intermediate.[22] However, the intermediate has not been detected, and the singlet energy transfer cannot occur under free diffusion conditions because of the short lifetime of the excited singlet state. Transient spectroscopies at high concentration will provide information on the mechanism of such concentration effects.

In the process of cis-to-trans isomerization, Φ_{tc-tt} (0.26) was higher than Φ_{cc-tc} (0.18). The relatively high value of Φ_{tc-tt} was explained by the steric distortion and the energy transfer (vide supra). The value of Φ_{cc-tc} was lower than the quantum yield of cis-to-trans isomerization ($\Phi_{c-t} = 0.35$)[23] in azobenzene. This might be due to the steric distortion in the transition state between **2**(c,c) and **2**(t,c) in the excited state. However, the mechanism does not seem to be simple because Φ_{cc-tc} is very high on 436-nm irradiation as described below.

(b) 436-nm Excitation. At 436 nm, Φ_{tt-tc} (0.34) was higher than Φ_{tc-cc} (0.15). This tendency was similar to the result of the 313-nm excitation. Φ_{tt-tc} is even higher than Φ_{t-c} (0.28) of azobenzene.[21,24] These results indicate that the transition state in the excited state has a very small activation barrier, or the other nonradiative decay processes such as internal conversion are suppressed by the bridges which limit the degree of freedom of the conformational change. In **2**(t,c), because the *cis*-azobenzene unit absorbs more photons than the *trans*-azobenzene unit on 436-nm irradiation, Φ_{tc-tt} (0.35) was higher than Φ_{tc-cc}. It is not clear that the energy transfer takes place from the *trans*- to *cis*-azobenzene unit upon n,π^* excitation because the individual absorptivities of the chromophores are uncertain. The photoisomerization from **2**(c,c) to **2**(t,c) was very efficient. The quantum yield ($\Phi_{cc-tc} = 0.51$) was close to that of the cis-to-trans isomerization of azobenzene ($\Phi_{c-t} = 0.50$).[21] It seems that the ring strain does not operate in the geometrical change from **2**(c,c) to **2**(t,c) in the S_1(n,π^*) state. This result is in contrast to that of the 313-nm excitation where Φ_{cc-tc} is low, and therefore, the **2**(c,c)-to-**2**(t,c) photoisomerization process is also dependent on the excitation wavelength. The reason for the dependency is that the mechanism of the cis-to-trans isomerization might depend on the

(21) Ronayette, J.; Arnaud, R.; Lebourgeois, P.; Lemaire, J. *Can. J. Chem.* **1974**, *52*, 1848−1857.

(22) Kojima, M.; Takagi, T.; Karatsu, T. *Chem. Lett.* **2000**, 686−687.

(23) Siampiringue, N.; Guyot, G.; Monti, S.; Bortolus, P. *J. Photochem.* **1987**, *37*, 185−188.

(24) Zimmerman, G.; Ghow, L.-Y.; Paik, U.-J. *J. Am. Chem. Soc.* **1958**, *80*, 3528−3531.

electronic state or that other nonradiative processes operate in a certain state.

(c) Photochemical Isomerization Mechanism. It has been well-known that there is a wavelength dependence in the quantum yield of the isomerization of azobenzene. In the process of the trans-to-cis isomerization, the quantum yield (Φ_{t-c}) is 0.10 at 313-nm irradiation,[21,24,25] while Φ_{t-c} is 0.28 at 436-nm irradiation.[21,24] This effect has been explained by the different reaction mechanisms in each electronic state: a rotation mechanism in the $S_2(\pi,\pi^*)$ state and an inversion mechanism in the $S_1(n,\pi^*)$ state. These mechanisms have been supported experimentally by the quantum yields of macrocyclic azobenzenes[6a,26] and azobenzenes with bulky substituents[5] and by theoretical calculations.[27] For example, **1a** shows almost no wavelength effect on the quantum yields for the photoisomerization from t,t to t,c. It was 0.24 on $S_1(n,\pi^*)$ excitation and 0.21 on $S_2(\pi,\pi^*)$ excitation.[6a] Rotation is suggested to be blocked by the ring strain in this compound. The quantum yields were almost equal because the internal conversion from $S_2(\pi,\pi^*)$ to $S_1(n,\pi^*)$ takes place without isomerization, and the isomerization proceeds via inversion along the $S_1(n,\pi^*)$ surface. These results have been believed to be powerful evidence of the occurrence of the inversion in the $S_1(n,\pi^*)$ state. In the case of **2**, however, the quantum yield for the isomerization of **2**(t,t)-to-**2**(t,c) (Φ_{tt-tc}) was 0.25 on 313-nm ($S_2(\pi,\pi^*)$) excitation, while 0.34 on 436-nm ($S_1(n,\pi^*)$) excitation. The difference between these values was beyond experimental error. To examine our experimental conditions, the quantum yields for the trans-to-cis isomerization (Φ_{t-c}) of 3,3′-dimethylazobenzene (**DMAB**) were measured under the same conditions for **2** and determined to be 0.16 and 0.30 on $S_2(\pi,\pi^*)$ (313 nm) and $S_1(n,\pi^*)$ (436 nm) excitation, respectively. These values are very close to the reported values for azobenzene.[21,24,25] From these results, it can be concluded that there is a wavelength dependence in the photoisomerization of **2**(t,t)-to-**2**(t,c) similar to that of the trans-to-cis isomerization in azobenzene. The results are in contrast to those that have been reported by Rau et al.[6a] If the rotation mechanism is inhibited in the trans-to-cis isomerization of **2**(t,t), there is no wavelength dependence in the quantum yield. From this viewpoint, one may say that the rotation is not blocked by the ring strain. There is further evidence that suggests that the ring strain cannot inhibit the rotation mechanism. A stilbenophane, where two stilbene units are connected by $-(CH_2)_2-$ chains at the para position, exhibited mutual photoisomerization around the C=C bond.[28] The quantum yield for the trans,trans-to-trans,cis isomerization was as high as 0.43.[28a] Stilbene is a well-known compound that isomerizes via rotation. Therefore, in azobenzenophanes, it seems impossible to exclude the rotation mechanism in the $S_1(n,\pi^*)$ state even if the azobenzene chromophore is fixed in its cyclic structure. Actually, it was possible to rotate the N=N double bonds from trans to cis and vice versa in the HKS molecular models. These facts indicate that both the rotation and inversion can operate in **2**.

As described above, the photoisomerization mechanism of azobenzene seemed to be well studied. Recent studies as well as our study, however, indicate that the trans-to-cis photoisomerization mechanism of azobenzene is not as simple as has been believed. For example, theoretical studies have suggested the possibility that the rotation mechanism in the $S_1(n,\pi^*)$ state cannot be ruled out, because there is a minimum in the midpoint of the rotation pathway, although the energy increases gradually in the inversion pathway in the trans-to-cis isomerization process.[29,30] An energy surface calculated by the CASSCF method has indicated that the isomerization does not occur by either mechanism in the $S_2(\pi,\pi^*)$ state where the trans isomer is very stable.[29] Moreover, transient Raman[31] and femtosecond fluorescence[32] spectroscopies have revealed that, on the $S_2(\pi,\pi^*)$ excitation, the isomerization proceeds via inversion in the highly vibrationally excited state of the $S_1(n,\pi^*)$ state after a very fast internal conversion. According to these recent studies, it seems that the isomerization along the $S_2(\pi,\pi^*)$ surface does not take place, although there are still discrepancies in the reaction mechanism from the $S_1(n,\pi^*)$ state between theoretical and experimental viewpoints. The wavelength dependence in the quantum yield of trans-to-cis isomerization in azobenzene might be attributable to the competition among several deactivation processes from the $S_2(\pi,\pi^*)$, such as internal conversion and geometrical change which do not contribute to the isomerization. The inversion and the rotation processes might be competing in the $S_1(n,\pi^*)$ state.

Complex with Alkali Metal Cations. It is well-known that macrocyclic compounds such as crown ethers and cryptands form inclusion complexes with alkali metal cations and that the selectivity of cations is dependent on the size of the molecular cavity.[33] The ion selectivity has been studied by electrospray ionization mass spectrometry (ESIMS), which is a powerful method for identification and characterization of weak interacting complexes.[34] For the complexations of a crown ether or a cryptand with alkali metal cations, the peak intensity of metal complexes obtained by ESIMS is in good correlation with the actual binding constants in solution.[35] For the azobenzenophanes, there is no evidence for the validity of the ESIMS for a quantitative estimation of the cation selectivity from the relative intensity. However, the relative peak intensity was employed for at least qualitative evaluation of the change in the cation selectivity of the azobenzenophanes.

In Figures 9−11, the intensity of the 1:1 complex with Cs^+ was increased in the order of **2**(t,t), **3**(t,t,t), and

(25) Yamashita, S.; Ono, H.; Toyama, O. *Bull. Chem. Soc. Jpn.* **1962**, *35*, 1849−1853.
(26) Rau, H. *J. Photochem.* **1984**, *26*, 221−225.
(27) Monti, S.; Orlandi, G.; Palmieri, P. *Chem. Phys.* **1982**, *71*, 87−99.
(28) (a) Anger, I.; Sandros, K.; Sundahl, M.; Wennerström, O. *J. Phys. Chem.* **1993**, *97*, 1920−1923. (b) Tanner, D.; Wennerström O. *Tetrahedron Lett.* **1981**, *22*, 2313−2316. (c) Rau, H.; Waldner, I. *Phys. Chem. Chem. Phys.* **2002**, *4*, 1776−1780.
(29) Ishikawa, T.; Noro, T.; Soda, T. *J. Chem. Phys.* **2001**, *115*, 7503−7512.
(30) Cattaneo, P.; Persico, M. *Phys. Chem. Chem. Phys.* **1999**, *1*, 4739−4743.
(31) Fujino, T.; Tahara, T. *J. Phys. Chem. A* **2000**, *104*, 4203−4210.
(32) Fujino, T.; Arzhantsev, S. Y.; Tahara T. *J. Phys. Chem. A* **2001**, *105*, 8123−8129.
(33) Vögtle, F. In *Supramolecular Chemistry: An Introduction*; John Wiley & Sons: Chichester, UK. 1989; Chapter 2.
(34) Schalley, C. A. *Int. J. Mass Spectrom.* **2000**, *194*, 11−39.
(35) Leize, E.; Jaffrezic, A.; Van Dorsselaer, A. *J. Mass Spectrom*, **1996**, *31*, 537−544.

4(t,t,t,t), which indicates that the complexation of the macrocycles with Cs^+ is on the inside of the cavity. But the intensity of the 1:1 complex with Rb^+ was decreased rather than increased with an increase in the ring size. Common hosts showing binding ability with Cs^+ tend to bind with Rb^+ because the difference in radius for Cs^+ (1.70 Å) and Rb^+ (1.49 Å) is not significant among alkali metal ions. This extraordinary tendency implies that the ion-selectivity does not depend simply on the ring size. On the other hand, it is reported that the π electrons for *trans*-azobenzene prefer to delocalize compared with the cis isomer.[16] This means that *trans*-azobenzene can be a softer host than the cis one. Therefore, the *trans*-azobenzene is expected to prefer a soft ion such as Cs^+. This assumption is consistent with the complex formation tendencies in which the relative intensity for the 1:1 and 2:1 complex is higher under the 436-nm irradiation than the 366-nm irradiation regardless of the ring size.

Without light irradiation, the relative intensity was highest at Cs^+ for all three azobenzenophanes. These facts indicate that the cavities are sufficiently large in **2**(t,t), **3**(t,t,t), and **4**(t,t,t,t). We are lacking definite information on the structure of the complex, because there is no evidence regarding whether the complexation is due to cation$-\pi$ interaction or to coordination between the cation and the lone pairs of N atoms. However, the cyclic structure plays an important role in the stabilization of the complex, because **DMAB** exhibited a very low intensity for the 1:1 complex with an alkali metal cation and showed no signals attributable to the 2:1 complex. The comparison with stilbene might give some information about the metal-ion binding site. The largest change in the selectivity before and after the photoirradiation was observed in **4**. Despite its very large ring size, the relative selectivity for small cations (Li^+ and Na^+) was increased by photoirradiation. From the isomer ratio at the photostationary state (Table 6), about 60% of the all-cis isomer (**4**(c,c,c,c)) exists in the solution after exposure to 366-nm irradiation. Although the type of interaction and the structure of the complex are uncertain, small cations probably bind to a local site of the macrocycle where azobenzene units are forced to be arranged closely due to trans-to-cis photoisomerization.[36]

Conclusion

The crystal structure analyses of all isomers of **2** revealed that the ring strain alters the rate of the thermal cis−trans isomerization of azobenzenophane. The compensation relationship between $\Delta H^{\ddagger}$ and $\Delta S^{\ddagger}$ showed that the thermal isomerization mechanism of **2** involved inversion. On the basis of the excitation wavelength dependence in the photochemical isomerization of **2**, rotation cannot be excluded for the photochemical isomerization of azobenzene in the $S_1(n,\pi^*)$ state. By covalently fixing two azobenzene moieties in the vicinity, the possibility of the intramolecular singlet energy transfer arises from the *trans*- to the *cis*-azobenzene unit. X-ray crystal structure analyses and ESIMS showed the possibility of photoresponsive host molecules which capture the cations or organic molecules.

(36) Pearson, R. G. *J. Am. Chem. Soc.* **1963**, *85*, 3533−3539.

Experimental Section

Materials. 3,3′-Dimethylazobenzene (commercially available) was recrystallized from methanol. Solvents for the spectroscopic measurements (acetonitrile and benzene) were spectroscopic grade.

Synthesis of 2, 3, and 4. A solution of bis(3-nitrophenyl)-methane[10] (5.0 g, 19 mmol) in dry 1,4-dioxane (400 mL) was added dropwise over 5 days to a suspension of $LiAlH_4$ (3.5 g, 91 mmol) in 1,4-dioxane (300 mL) under a nitrogen atmosphere at 100 °C. After the reaction mixture was cooled to 0 °C, water (200 mL) was carefully added. The precipitate was filtered off and the solvent was removed by evaporation. The residual orange solid was taken up in dichloromethane, and the solution was washed with water and evaporated. The residue was isolated by silica gel column chromatography, preparative TLC, and gel permeation chromatography (GPC). The column used for GPC was Shodex KF-2002.5 with THF.

***trans,trans*-[1.1](3,3′)-Azobenzenophane (2(t,t)):** Yield 9.5 mg (0.13%), mp 165.5−165.9 °C. ^{1}H NMR (600 MHz, $CDCl_3$) δ 8.16 (s, 4H), 7.66 (d, J = 7.7 Hz, 4H), 7.38 (t, J = 7.7 Hz, 4H), 7.34 (d, J = 7.7 Hz, 4H), 4.18 (s, 4H). ^{13}C NMR (75 MHz, $CDCl_3$) δ 153.67, 140.86, 131.08, 129.21, 125.97, 118.91, 40.17. HRMS (m/z) calcd for $C_{26}H_{20}N_4$ 388.1687, found 388.1713. ESIMS (m/z) $[M + H]^+$ calcd for $C_{26}H_{21}N_4$ 389.18, found 389.12.

***trans,trans,trans*-[1.1.1](3,3′)-Azobenzenophane (3(t,t,t)):** Yield 20 mg (0.18%), mp 283.9−284.6 °C. ^{1}H NMR (600 MHz, $CDCl_3$) δ 7.71 (d, J = 7.7 Hz, 6H), 7.69 (s, 6H), 7.43 (t, J = 7.7 Hz, 6H), 7.39 (d, J = 7.7 Hz, 6H), 4.12 (s, 6H). ^{13}C NMR (75 MHz, $CDCl_3$) δ 153.17, 142.10, 131.63, 129.30, 122.95, 121.28, 41.78. HRMS (m/z) calcd for $C_{39}H_{30}N_6$ 582.2530, found 582.2584. ESIMS (m/z) $[M + H]^+$ calcd for $C_{39}H_{31}N_6$ 583.26, found 583.30.

***trans,trans,trans,trans*-[1.1.1.1](3,3′)-Azobenzenophane (4(t,t,t,t)):** Yield 39 mg (0.26%), mp 294.2−294.4 °C. ^{1}H NMR (600 MHz, $CDCl_3$) δ 7.72 (d, J = 7.7 Hz, 8H), 7.67 (s, 8H), 7.41 (t, J = 7.7 Hz, 8H), 7.32 (d, J = 7.7 Hz, 8H), 4.14 (s, 8H). ^{13}C NMR (75 MHz, $CDCl_3$) δ 153.05, 141.75, 131.71, 129.25, 123.44, 120.95, 41.43. ESIMS (m/z) $[M + H]^+$ calcd for $C_{52}H_{41}N_8$ 777.35, found 777.42.

X-ray Crystallographic Data. Crystal data for 2(t,t): $C_{26}H_{20}N_4$, M = 388.46, monoclinic, $P2_1$, a = 10.409(2) Å, b = 16.274(2) Å, c = 12.299(3) Å, β = 101.256(9)°, V = 2043.3(6) Å^3, Z = 4, D_{calc} = 1.263 g/cm^3, crystal size 0.27 × 0.17 × 0.07 mm^3. Diffraction data were collected at 296 K on an Enraf-Nonius CAD4 diffractometer with Cu Kα radiation. The structure was solved by direct methods and refined by a full-matrix least-squares analysis. All calculations were performed with the teXsan crystallographic software package. $R1$ = 0.081 and Rw = 0.203 (based on F^2).

Crystal data for 2(t,c): $C_{26}H_{20}N_4$, M = 388.46, orthorhombic, $P2_12_12_1$, a = 11.096(3) Å, b = 40.91(2) Å, c = 9.121(2) Å, V = 4140(2) Å^3, Z = 8, D_{calc} = 1.246 g/cm^3, crystal size 0.30 × 0.07 × 0.03 mm^3. Diffraction data were collected at 243 K on a Rigaku AFC7R diffractometer with Mo Kα radiation. The structure was solved by direct methods and refined by a full-matrix least-squares analysis. All calculations were performed with the teXsan crystallographic software package. $R1$ = 0.044 and Rw = 0.154 (based on F^2).

Crystal data for 2(c,c): $C_{26}H_{20}N_4$, M = 388.46, orthorhombic, $Fddd$, a = 17.009(2) Å, b = 27.519(3) Å, c = 8.500(2) Å, V = 3978.5(10) Å^3, Z = 8, D_{calc} = 1.297 g/cm^3, crystal size 0.20 × 0.20 × 0.10 mm^3. Diffraction data were collected at 243 K on a Rigaku AFC7R diffractometer with Mo Kα radiation. The structure was solved by direct methods and refined by a full-matrix least-squares analysis. All calculations were performed with the teXsan crystallographic software package. $R1$ = 0.038 and Rw = 0.121 (based on F^2).

Crystal data for 3(t,t,t): $C_{39}H_{30}N_6{\cdot}CHCl_3$, M = 702.06, trigonal, $R3c$, a = 25.217(3) Å, c = 9.380(3) Å, V = 5166(2) Å^3, Z = 6, D_{calc} = 1.354 g/cm^3, crystal size 0.50 × 0.10 × 0.05 mm^3. Diffraction data were collected at 223 K on a Rigaku AFC7R diffractometer with Mo Kα radiation. The structure was solved

by direct methods and refined by a full-matrix least-squares analysis. All calculations were performed with the teXsan crystallographic software package. $R1 = 0.083$ and $Rw = 0.211$ (based on F^2).

Crystal data for 4(t,t,t,t): $C_{52}H_{40}N_8 \cdot CH_2Cl_2$, $M = 861.84$, monoclinic, $C2/c$, $a = 26.833(6)$ Å, $b = 6.391(1)$ Å, $c = 28.216(5)$ Å, $\beta = 111.89(2)°$, $V = 4489(1)$ Å^3, $Z = 4$, $D_{calc} = 1.275$ g/cm^3, crystal size $0.50 \times 0.03 \times 0.06$ mm^3. Diffraction data were collected at 243 K on a MAC Science MXC18K diffractometer with Mo Kα radiation. The structure was solved by direct methods and refined by a full-matrix least-squares analysis. All calculations were performed with the teXsan crystallographic software package. $R1 = 0.053$ and $Rw = 0.167$ (based on F^2).

Instrumentation. Melting points (uncorrected) were determined on a hot stage equipped with an optical microscope. ^{1}H NMR spectra were recorded on a 270-, 300-, or 600-MHz spectrometer. ^{13}C NMR spectra were recorded on a 75-MHz spectrometer. UV−vis absorption spectra were measured by a double-beam spectrophotometer. Ratios of the isomers were examined by HPLC. Columns used for HPLC were ODS-80Ts (TOSO Co.), with methanol for the analysis of **2**, and CN-80Ts (TOSO Co.), with ethyl acetate/hexane = 25/75 for the analyses of **3** and **4**. Under those conditions, peaks attributable to **2**(t,t), **2**(t,c), and **2**(c,c) appeared at 6.2, 3.3, and 2.5 min, respectively. Peaks of **3**(t,t,t), **3**(t,t,c), **3**(t,c,c), and **3**(c,c,c) appeared at 4.7, 6.1, 8.4, and 10.3 min, respectively. Peaks of **4**(t,t,t,t), **4**(t,t,t,c), **4**(t,t,c,c), **4**(t,c,t,c), **4**(t,c,c,c), and **4**(c,c,c,c) appeared at 5.0, 6.7, 8.5, 8.9, 13.3, and 19.2 min, respectively. Photoirradiation was carried out with a 150-W xenon lamp with a monochromator with a bandwidth of ca. 3 nm for all wavelengths used for the experiments. HRMS was measured on a Hitachi M80B mass spectrometer. ESIMS was performed on a Mariner (Applied Biosystems) mass spectrometer. General instrument settings for ESIMS are as follows: vaporizing temperature, 140 °C; infusion rate, 3 μL min^{-1}; capillary voltage, 3100 V; nozzle potential, 100 V. The signal intensities were averaged over five scans and recorded as the sum of the corresponding isotopic peaks.

Quantum Yield for Isomerization. At first, the quantum yield of the isomerization from **2**(t,t) to **2**(t,c) (Φ_{tt-tc}) was obtained by determining the amount of **2**(t,c) by HPLC upon photoirradiation of **2**(t,t). The conversion of **2**(t,t) was kept below 5% to avoid the error caused by the absorption by **2**(t,c). The light quanta absorbed by the sample was determined by potassium ferrioxalate actinometer. The other quantum yields, Φ_{tc-tt}, Φ_{tc-cc}, and Φ_{cc-tc}, were determined by the following equations with use of Φ_{tt-tc}, ϵ, and the ratio at the photostationary state in Table 3. On photoirradiation, the change in the concentration ([tt], [tc], and [cc]) of each isomer is defined as:

$$\frac{d[tt]}{dt} = -I_0(1 - 10^{-D}) \times \frac{\epsilon_{tt}[tt]l}{D} \times \frac{1}{V} \times \Phi_{tt-tc} + I_0(1 - 10^{-D}) \times \frac{\epsilon_{tc}[tc]l}{D} \times \frac{1}{V} \times \Phi_{tc-tt} + k_2[tc] \quad (1)$$

$$\frac{d[tc]}{dt} = -I_0(1 - 10^{-D}) \times \frac{\epsilon_{tc}[tc]l}{D} \times \frac{1}{V} \times \Phi_{tc-tt} - I_0(1 - 10^{-D}) \times \frac{\epsilon_{tc}[tc]l}{D} \times \frac{1}{V} \times \Phi_{tc-cc} + I_0(1 - 10^{-D}) \times \frac{\epsilon_{tt}[tt]l}{D} \times \frac{1}{V} \times \Phi_{tt-tc} + I_0(1 - 10^{-D}) \times \frac{\epsilon_{cc}[cc]l}{D} \times \frac{1}{V} \times \Phi_{cc-tc} + k_2[cc] - k_2[tc] \quad (2)$$

$$\frac{d[cc]}{dt} = -I_0(1 - 10^{-D}) \times \frac{\epsilon_{cc}[cc]l}{D} \times \frac{1}{V} \times \Phi_{cc-tc} + I_0(1 - 10^{-D}) \times \frac{\epsilon_{tc}[tc]l}{D} \times \frac{1}{V} \times \Phi_{tc-cc} - k_2[cc] \quad (3)$$

where I_0, D, ϵ, and V are the initial intensity of light, the absorbance of the sample, the molar extinction coefficient at the excitation wavelength, and the volume of the sample solution, respectively. The terms for the thermal isomerization are neglected because the lifetimes of both **2**(c,c) and **2**(t,c) were sufficiently longer than the period of time for the measurement (several hours). At the photostationary state, $d[tt]/dt = d[tc]/dt = d[cc]/dt = 0$, eqs 1−3 can be rewritten as eqs 4−6.

$$-\epsilon_{tt}[tt]\Phi_{tt-tc} + \epsilon_{tc}[tc]\Phi_{tc-tt} = 0 \quad (4)$$

$$-\epsilon_{tc}[tc]\Phi_{tc-tt} - \epsilon_{tc}[tc]\Phi_{tc-cc} + \epsilon_{tt}[tt]\Phi_{tt-tc} + \epsilon_{cc}[cc]\Phi_{cc-tc} = 0 \quad (5)$$

$$-\epsilon_{cc}[cc]\Phi_{cc-tc} + \epsilon_{tc}[tc]\Phi_{tc-cc} = 0 \quad (6)$$

From eq 4, we can obtain eq 7, where [tc]/[tt] is equal to the isomer ratio at the photostationary state (Table 3). The value of $\epsilon_{tc}/\epsilon_{tt}$ was determined by HPLC by comparing the area of the isomers of known concentration. Thus, the value of Φ_{tc-tt} was obtained by using the value of Φ_{tt-tc}, which has been measured directly.

$$\frac{\Phi_{tt-tc}}{\Phi_{tc-tt}} = \frac{\epsilon_{tc}}{\epsilon_{tt}} \frac{[tc]}{[tt]} \quad (7)$$

$$\frac{\Phi_{cc-tc}}{\Phi_{tc-cc}} = \frac{\epsilon_{tc}}{\epsilon_{cc}} \frac{[tc]}{[cc]} \quad (8)$$

Similarly, eq 6 can be rewritten as eq 8; however, both Φ_{tc-cc} and Φ_{cc-tc} are unknown values and eq 8 gives only the ratio of these values. Another equation is required to obtain these values. As for the 313-nm irradiation, $d[tc]/dt = 0$ at $t = 32$ min in Figure 7a, and eq 9 is obtained under this condition:

$$-\epsilon_{tc}[tc]'\Phi_{tc-tt} - \epsilon_{tc}[tc]'\Phi_{tc-cc} + \epsilon_{tt}[tt]'\Phi_{tt-tc} + \epsilon_{cc}[cc]'\Phi_{cc-tc} = 0 \quad (9)$$

where [tt]′, [tc]′, and [cc]′ are the concentration of each isomer at $t = 32$ min. Finally, Φ_{tc-cc} and Φ_{cc-tc} are determined by solving eqs 8 and 9. As for the 436-nm irradiation, there was no maximum point ($d[tc]/dt = 0$) of **2**(t,c) on the irradiation of **2**(t,t). Thus, the condition where $d[tc]/dt = 0$ at $t = 25$ min in Figure 7b was used to determine the values of Φ_{tc-cc} and Φ_{cc-tc}.

Quantum Chemical Calculations. All optimized structures of **2**(t,t), **2**(t,c), and **2**(c,c) were obtained by full-optimization with use of the GAUSSIAN 98 program package.[15] The atomic coordinates of the crystal structure were used as the initial structure. Semiempirical calculation (AM1) was carried out with the CAChe WorkSystem Ver. 5.02 on a Windows computer.

Acknowledgment. We thank Ms. Midori Goto for the X-ray crystallography and Ms. Ritsuko Nagahata for her assistance in the mass spectrometry experiments. We also thank TACC (Tsukuba Advanced Computing Center) for providing us the calculation facilities. Y.N. thanks NEDO (New Energy and Industrial Technology Development Organization) for the fellowship.

Supporting Information Available: Crystal data for **2**(t,t), **2**(t,c), **2**(c,c), **3**(t,t,t), and **4**(t,t,t,t) (CIF) and ^{1}H NMR and ^{13}C NMR spectra of **2**(t,t), **3**(t,t,t), and **4**(t,t,t,t). This material is available free of charge via the Internet at http://pubs.acs.org.

JO0341160